

Astrophysical background and dark matter implication based on latest AMS-02 data

Hong-Bo Jin^{a,b*}, Yue-Liang Wu^{a,c,d†} and Yu-Feng Zhou^{a,c,d‡}

^a *CAS Key Laboratory of Theoretical Physics, Chinese Academy of Sciences*

^b *National Astronomical Observatories, Chinese Academy of Sciences, Beijing, 100012, China*

^c *Institute of Theoretical Physics, Chinese Academy of Sciences, Beijing 100190, China*

^d *University of Chinese Academy of Sciences, Beijing 100190, China*

Abstract

The cosmic ray (CR) positrons and antiprotons are often regarded as the products of collisions of CR nucleons with the interstellar medium. However this conclusion is challenged by recent experimental data. In this work, we choose the latest AMS-02 data to analyze the astrophysical background of CR positrons and antiprotons based on the GALPROP code for CR propagation and QGSJET-II-04 for hadronic CR interactions. The results show that in low energy the flux of CR antiprotons is consistent with AMS-02 data, and the over-predicted flux of CR positrons is well reduced in a diffusion model combining the re-acceleration and convection terms. Using this model, the calculated flux of CR protons is consistent with AMS-02 data with the hardening feature above 330 GeV. Based on this model, using the total fluxes of CR electrons and positrons from AMS-02, interpretation of dark matter annihilation on the positron excess are also analyzed.

*Email: hbjin@bao.ac.cn

†Email: ylwu@itp.ac.cn

‡Email: yfzhou@itp.ac.cn

1 Introduction

In the origin of Galactic CRs, the primary particles, such as nucleons and electrons, are commonly regarded as the injection of Supernova relics(SNRs), in which, CRs are accelerated by the diffusive shock [1–5]. In this mechanism, the injection spectra of CRs are a power law below Knee, which are verified by the experimental data [6]. The other particles called as the secondary CRs, are mainly produced in the collision between the primary particles and the interstellar medium in the Galaxy. In the analysis of the secondary CRs, the collision cross-sections between them are often calculated with the hadronic interaction models. Since the spectra of the primary CRs are a single power law, the spectral features of the secondary CRs, deriving the origin of CRs, are mainly relevant to the hadronic interaction models. Besides the hadronic interaction models, the exclusive cross-section of the produced particles are also calculated with the empirical parameterizations of the accelerator data. In practice, these calculations are often performed using Monte Carlo(MC) event generators, and combining the accelerator data, which are developed into the parameterization model package, such as FLUKA [7, 8], QGSJET-II-04 [9], EPOS-LHC [10], etc. In this paper, QGSJET-II-04 is chosen to calculate the secondary antiproton product.

When the charged particles of CRs propagate in the Galaxy, they may be accelerated via the interaction with the turbulent interstellar magnetic field, which is also called as re-acceleration in contrast to DSA. On the meantime, CRs may commit the energy loss when propagating in the Galactic winds, which are blowing outwards from the Galactic disc. That is called as convection in CR propagation models. Besides the Galactic diffusion of CRs, these interactions alter the original structure of the spectra of CRs. As a result, the measured spectra of CRs are different from the injection of the sources. Thus, the uncertainties of the secondary particle spectra are also from the propagation models of CRs. In the conventional model, CR production and propagation are governed by the same mechanism at energies below 10^{17} eV, and CR propagation is often described by the diffusion equation [11]. Thus, based on the propagation models and the hadronic interaction models, the astrophysical spectra of the secondary particles are predicted with the experimental data of the primary particles of CRs.

Recently, AMS-02 reported their observed results of cosmic rays. Below TeV, the spectra of CR protons can be described by the high precision data [12]. CR positrons [13], antiprotons [14] and B/C [15] have also precise measurements. In our previous analysis [16], we have performed a global analysis of CR propagation parameters with the only AMS-02 data. The propagation parameters have been shown to be well determined by the only CR proton and B/C data of AMS-02, which is the first strategy of fitting parameters different from the two ratios of CRs, such as $\text{Be}^9/\text{Be}^{10}$ and B/C. The con-

strained parameters of the proton and B/C case have very narrow range at the 95% confidence level(CL) and are also less than the $\text{Be}^9/\text{Be}^{10}$ and B/C case in the same CL. Based on the propagation parameter models constrained by the measured data of CRs, the astrophysical spectra of the secondary particles are naturally predicted in a given CL. Since the astrophysical spectra of the secondary particles, such as CR positrons [13] and antiprotons [14], already have the measured data with high precision, the predicted spectra of them may be used to verify the propagation model and explore the origin of the experimental data. The positron excess has been discovered by PAMELA [17], Fermi-LAT [18] and AMS-02 [19] in the past years, which indicated that above 10 GeV the CR positron fluxes of experimental data are greater than the astrophysical fluxes predicted by the CR propagation models and the hadronic interaction models. The phenomenological implications can be found in refs. [16, 20–23]

Below 10 GeV the astrophysical fluxes of CR positrons and antiprotons analyzed based on the current models are actually both inconsistent with the latest data of AMS-02, i.e. the fluxes of CR positrons are greater than the measured data and the fluxes of antiprotons are less than that data. Authors in [24] made predictions for the CR positrons and antiprotons from a global bayesian analysis by using GALPROP package [25], the resulted fluxes were also found to be inconsistent with the experimental data below 10 TeV. It indicated that the under-predicted antiprotons may result from a general feature of the re-acceleration models. Furthermore, the uncertainties of the antiproton flux have been analyzed sufficiently in ref. [26, 27], which involves the cross-section of interaction between nucleons, the propagation of CRs, solar modulation and the spectral slope of the primary CRs. As a result, there are some of those parameters that may predict the consistent flux of antiproton with AMS-02 data. While there were no concerned figures and χ^2 presented to indicate whether these parameters could also lead to a well prediction for the flux of protons and B/C ratio in ref. [26]. The similar analysis is also found in ref. [28]. In the analyses [29–32], the under-predicted antiprotons were considered as the possible evidence of a new primary component of CR antiprotons. Another possible excess can be found at high energies around 300 GeV [33].

In this paper, the analysis strategy of CR positrons and antiprotons is the following. The calculations of the cross-section relevant to producing antiprotons between the interstellar medium and the primary CRs, are performed by Monte Carlo (MC) generator QGSJET-II-04 [9]. The strategy of the calculations is to make a parameterization for the results in ref. [34]. In the source term of propagation equation, the injection spectra of the primary CRs is characterized by a continuous function in the referred rigidity of CRs instead of a broken power law, which is useful to fit the features of the measured spectra of CRs by Voyager [35, 36] and analytically express a simple power law with the same

indices below/above the referred rigidity. In the propagation models, the re-acceleration and convection of the Galactic CRs are both taken into account. The propagation equation of CRs is solved numerically using GALPROP package [25]. The effect of the solar modulation of CRs is considered using the model of force-field approximation [37].

Based on the analysis strategy in the context, the under-predicted flux of CR antiprotons, has been intensified to be consistent with the AMS-02 data [14] in the re-acceleration diffusion model. Such a consistency results from the recalculation of antiproton production in the nucleon collision by using MC generators and Z-factors [34, 38]. While the predicted flux of CR positrons below 10 GeV is not automatically consistent with the AMS-02 data [13] in this re-acceleration diffusion model. And the over-predicted flux of CR positrons below 10 GeV cannot be reduced by just adding the exclusive potential of the solar modulation for CR positrons or adjusting the propagation parameters at the larger CL, favored by the experimental data of CR protons, and B/C ratio. We show that only by combining the convection and re-acceleration diffusion models, the over-predicted flux of CR positrons can be depressed and meantime the flux of CR antiprotons can also become consistent with the AMS-02 data. The following sections will illustrate the details of the analysis concerned.

This paper is organized as follows. In section 2, we outline the framework for the calculation of the propagation of the cosmic-ray particles and the cross-section of interaction between nucleons. In section 3, we describe the data selection and the strategy of the data fitting in a number of propagation models. The numerical results are presented in section 4. Our conclusions are given in section 5.

2 Cosmic ray propagation and the secondary particle production in the interstellar medium

In the conventional model, CR production and propagation are governed by the same mechanism at energies below 10^{17} eV. CR propagation is often described by the diffusion equation [11]:

$$\begin{aligned} \frac{\partial \psi}{\partial t} = & \nabla(D_{xx} \nabla \psi - \mathbf{V}_c \psi) + \frac{\partial}{\partial p} p^2 D_{pp} \frac{\partial}{\partial p} \frac{1}{p^2} \psi - \frac{\partial}{\partial p} \left[\dot{p} \psi - \frac{p}{3} (\nabla \cdot \mathbf{V}_c) \psi \right] \\ & - \frac{1}{\tau_f} \psi - \frac{1}{\tau_r} \psi + q(\mathbf{r}, p), \end{aligned} \quad (1)$$

where $\psi(\mathbf{r}, p, t)$ is the number density per unit of total particle momentum, which is related to the phase space density $f(\mathbf{r}, p, t)$ as $\psi(\mathbf{r}, p, t) = 4\pi p^2 f(\mathbf{r}, p, t)$. D_{xx} is the

spatial diffusion coefficient parametrized as

$$D_{xx} = \beta D_0 \left(\frac{\rho}{\rho_0} \right)^{\delta_{1,2}}, \quad (2)$$

where $\rho = p/(Ze)$ is the rigidity of the CR particles, and $\delta_{1(2)}$ is the index below (above) a reference rigidity ρ_0 . The parameter D_0 is a normalization constant and $\beta = v/c$ is the ratio of the velocity v of the CR particles to the speed c of light. \mathbf{V}_c is the convection velocity related to the drift of CR particles from the Galactic disc due to the Galactic wind. The diffusion in momentum space is described by the re-acceleration parameter D_{pp} related to the Alfvén speed V_a , i.e. the velocity of turbulences in the hydrodynamical plasma, whose level is characterized as ω [11, 39]:

$$D_{pp} = \frac{4V_a^2 p^2}{3D_{xx}\delta_i(4 - \delta_i^2)(4 - \delta_i)\omega}, \quad (3)$$

where $\delta_i = \delta_1$ or δ_2 is the index of the spatial diffusion coefficient. \dot{p} , τ_f and τ_r are the momentum loss rate, the time scales for fragmentation and the time scales for radioactive decay, respectively. The momentum loss rate of CR electrons is not the same as CR nucleons, and the relevant expressions are found in the APPENDIX C of paper [40].

The convection term in the equation(1) is used to describe the Galactic wind blowing outwards from the Galactic disc, and in the GALPROP [40], the wind velocity \mathbf{V}_c is expressed as [40]:

$$V_c = V_0 + z \frac{dV_c}{dz}, \quad (4)$$

z is the height perpendicular to the Galactic disc and also appears in the next equation (5).

The source $q(\mathbf{r}, p)$ of the primary particles is often described as a broken power law spectrum multiplied by the assumed spatial distribution described in the cylindrical coordinate (R, z) [40]:

$$q_A(R, z) = q_0 c_A \left(\frac{\rho}{\rho_{br}} \right)^{\gamma_s} \left(\frac{R}{R_\odot} \right)^\eta \exp \left[-\xi \frac{R - R_\odot}{R_\odot} - \frac{|z|}{0.2 \text{ kpc}} \right], \quad (5)$$

where $\eta = 0.5$, $\xi = 1.0$ and the parameter q_0 is normalized with the propagated flux of CR protons. c_A is the relative abundance of the A th nucleon. The reference rigidity ρ_{br} is described as the breaks of injection spectrum. γ_s is the power indices below(above) a reference rigidity.

In this paper, the injection spectra of the primary CRs is described by the expression of the continuous functions in the referred rigidity of CRs, which may express a simple

power law with the same indices below/above the referred rigidity. The expression $(\frac{\rho}{\rho_{br}})^{\gamma_s}$ is replaced by the following,

$$\left(\frac{\rho}{\rho_{br}}\right)^{-\gamma_1} \left(1 + \left(\frac{\rho}{\rho_{br}}\right)^{\frac{-\gamma_1 - (-\gamma_2)}{\alpha}}\right)^{-\alpha}, \quad (6)$$

γ_1 and γ_2 are the spectral indices below/above the referred rigidity, α determines the smoothness of the spectral change in the left and right sides of the referred rigidity, when α is 0, as a broken power law, the expression is same as the one in the equation (5). In this work, α is taken as a free parameter to analyze the smoothness of the injection spectra of CR nucleons.

The flux of secondary particles is derived from the primary particle's spectra, spatial distribution and interaction with the interstellar medium. The calculation of secondary particle flux is referred to the refs. [40, 41].

CR antiprotons and positrons are produced in the collision with the interstellar medium, and in the propagation equation(1) their source terms are described as follows [42],

$$q_{\bar{p}, e^\pm}(p) = \frac{c}{4\pi} \frac{dn(p)}{dt} = \frac{c}{4\pi} \sum_{i=H, He} n_i \sum_j \int dp' \beta n_j(p') \frac{d\sigma_{ij}(E_{tot}, p')}{dE_{tot}}, \quad (7)$$

n_i is the interstellar H and He density, $n_j(p')$ is density of No. j CR nucleon, and σ_{ij} is cross-section between the No. j CR nucleon and interstellar H and He.

Based on the cross-sections between the nucleon's collision, which are taken from the theoretical models or the collision experimental data, the equation(7) is often used to calculate the flux of secondary CRs. Recently, these calculations are improved by using Z-factors [34, 38], where they took a numerical calculation instead of using an equation(7). The concerned details can be found in the papers [34, 38]. For the Z-factors expression of CR antiproton case, the equation is modified as:

$$q_{\bar{p}}^{ij}(E_{\bar{p}}) = n_i I_j(E_{\bar{p}}) Z_{\bar{p}}^{ij}(E_{\bar{p}}, \alpha_j), \quad (8)$$

Here, α_j is the power index of the interstellar spectra $I_j(E_{\bar{p}}) \propto E_{\bar{p}}^{-\alpha_j}$ of No. j CR nucleon. the Z-factor $Z_{\bar{p}}^{ij}$ is expressed, via the inclusive spectra of antiprotons $d\sigma^{ij \rightarrow \bar{p}}(E, z_{\bar{p}})/dz_{\bar{p}}$ with $z_{\bar{p}} = E_{\bar{p}}/E$, as follows

$$Z_{\bar{p}}^{ij}(E_{\bar{p}}, \alpha_j) = \int_0^1 dz z^{\alpha-1} \frac{d\sigma^{ij \rightarrow \bar{p}}(E_{\bar{p}}/z, z)}{dz}. \quad (9)$$

In the Table(1) of paper [34], Z-factors are calculated with the modified QGSJET-II model, whose values are listed discretely in the limited ranges of the energy and the

spectral index. In the calculation of secondary particle's spectra, these numbers are not used conveniently. In this paper, these numbers are interpolated and fitted into an analytic expression, which can be written in a good approximation as continuous functions in the following,

$$\sigma_j(\epsilon_{\bar{p}}, \gamma_j) = \gamma_j^{-6} \ln^{0.8} [0.16 \epsilon_{\bar{p}} (10 - \ln A_j) + 1] \left(1 + \frac{1}{\epsilon_{\bar{p}}} + \frac{a}{\epsilon_{\bar{p}}^3}\right)^{-2}. \quad (10)$$

Where, the dimensionless quantity $\epsilon_{\bar{p}} = \frac{E_{\bar{p}}}{\text{GeV/n}}$ denotes kinetic energy $E_{\bar{p}}$ over GeV per nucleon. The spectral index α_j is replaced by γ_j , which is used in the equation (5) and (6). A_{gas}^i and A_j are the nucleon number of the i th interstellar gas and the j th CR nucleon respectively. $a=0.5$ when $A_j \leq 4$ and $a=1.0$ when $A_j > 4$.

With the equation (10), $Z_{\bar{p}}^{ij}(\epsilon_{\bar{p}}, \gamma_j)$ can simply be rewritten as,

$$Z_{\bar{p}}^{ij}(\epsilon_{\bar{p}}, \gamma_j) = C^{ij} A_{gas}^i A_j \sigma_j(\epsilon_{\bar{p}}). \quad (11)$$

Where, C^{ij} is a discrete function expressed as

$$C^{ij} = \begin{cases} 9.44, & A_{gas}^i = 1 \\ 8.97, & A_{gas}^i = 4, A_j = 1 \\ 7.08, & A_{gas}^i = 4, A_j > 1 \end{cases} \quad (12)$$

Based on the analytic expression (11), the updated source term of the secondary antiproton is expressed as,

$$q_{\bar{p}}(E_{\bar{p}}) = \sum_{i=H, He} n_i \sum_{j=1}^{A_{max}} I_j(E_{\bar{p}}) Z_{\bar{p}}^{ij}(E_{\bar{p}}, \gamma_j), \quad (13)$$

A_{max} is the maximum nucleon number of the chosen particle of CRs, which mainly contribute to the production of CR antiprotons. In order to check the values of the equation (11), an example is calculated and listed in Table 1. If σ is 0.02, the total χ^2 over data points between the equation (11) and reference [34] are near 1.0 for all cases (A_{gas}^i, A_j). Thus, the errors may be accepted.

In this paper, the CR propagation equation (1) is solved by GALPROP v54 package, which is based on a Crank-Nicholson implicit second-order scheme [40]. In order to solve the equation, a cylindrically symmetric geometry is assumed. And the spatial boundary conditions assume that the density of CR particles vanishes at the boundaries of radius R_h and half-height Z_h .

At the top of the atmosphere of the Earth, CR particles are affected by solar winds and the heliospheric magnetic field. The force-field approximation is used to describe this effect and the solar modulation potential ϕ denotes the force field intensity [37]. In this paper, ϕ is a free parameter and the difference of ϕ between the experimental data is taken for granted.

$E_{\bar{p}}$	(A_{gas}^i, A_j) in this paper Eq.(11)				(A_{gas}^i, A_j) in Ref. [34]			
	(P,P)	(P,He)	(He,P)	(He,CNO)	(P,P)	(P,He)	(He,P)	(He,CNO)
1	0.008	0.028	0.025	0.189	0.00772	0.0248	0.0277	0.196
10	0.094	0.360	0.310	3.617	0.1	0.35	0.339	3.24
100	0.178	0.694	0.587	7.106	0.187	0.715	0.612	7.15
1000	0.244	0.960	0.805	9.902	0.248	0.978	0.787	9.81
10000	0.304	1.199	1.002	12.428	0.307	1.2	0.959	12

Table 1: Z-factor calculated by Equation (11) and Ref. [34]. γ_j is chosen as 2.4 for the injection nucleons A_j , which is equal to the values in Table 1 of Ref. [34]. As an example, the A_j is 14 for CNO. The target nucleons A_{gas}^i are P and He.

3 Data selection and fitting schemes

In our previous paper [16], it was found that the propagation parameters: half-height Z_h , diffuse parameters D_0 and δ ($\delta = \delta_{1,2}$), Alfvén speed V_A , and power indices: $\gamma_{1,2}^p$ below(above) a reference rigidity ρ_{br} of CR protons, can be determined alone by the AMS-02 data: proton flux (P) and the ratio of Boron to Carbon flux (B/C) [16]. Thus, based on these parameters constrained from the AMS-02 data, the flux of the secondary CRs can be predicted. In this paper, in order to constrain the flux of CR antiprotons and positrons, besides the AMS-02 data of P and B/C, we shall also include the latest released AMS-02 data of CR antiprotons and positrons. It is already known that in the re-acceleration diffuse model, the flux of CR positrons below 10 GeV are over-predicted, which implies that the other effects of CRs propagation and interaction should be considered. These include the solar modulation ϕ and the convection effect, i.e. Galactic winds blowing outwards from the Galactic disc, which is denoted by V_c and dV_c/dZ_h in the context. Besides the smoothness parameter α in the Equation (6), there are in general 12 fitting parameters: $Z_h, D_0, \delta, V_A, \gamma_1^p, \gamma_2^p, \rho_{br}^p, N_p$ (Normalization of CR flux), $V_c, dV_c/dZ_h, \phi$ and α , which are determined from fitting four groups of AMS-02 data: Proton [12], B/C [15], antiproton [14] and positron [13]. Considering the background excess of CR positron, the energy range of the fitting to CR positron is limited in 0.6 GeV - 6.0 GeV, and also the energy range of CR antiproton flux is restricted to be in 2.0 GeV - 6.0 GeV due to the background excess of CR antiprotons from AMS-02 data. The low energy feature of CR antiprotons is derived from the hadronic interaction model. The concerned details can be found in Table 1 or in ref. [34].

With the 12 parameters and four groups of AMS-02 data, the parameter models are constructed to analyze the constrained flux of CR antiprotons and positrons from

AMS-02 data. The results are presented in Tables 3 and 4. In Table 3 and 4, DCR denotes for a diffusion model including the convection and re-acceleration effects, DR for a diffusion model involving only the re-acceleration effect, and DC for a diffusion model containing only the convection effect. In the DR model, the solar modulation potential ϕ is taken with different values for CR positrons and CR nucleons. In the DCR model, some hadronic models are improved to replace the equation (11). In order to compare the recalculated flux of CR antiprotons, a DCR model denoted as DCR₀ model is included, which takes the conventional hadronic models [43] with the corresponding best-fit parameters. In the DCR model, Alfvén speed V_A is not different between CR positrons and CR nucleons. The DCR_V model is constructed to verify whether re-acceleration has the different effect between CR positrons and CR nucleons.

For the dark matter implications of the AMS-02 data, the prediction of mass and annihilation cross-section of dark matter are based on the background of the total CR electrons and CR antiprotons, whose fluxes are calculated with the above best-fit parameters from the constraints of AMS-02 data. The fluxes of CR electrons are divided into the primary and secondary ones. In ref. [44], by using the re-acceleration diffusion model of CRs, the flux of primary electrons are predicted by the difference between CR electron and positron of the AMS-02 data. In this paper, the propagation parameters are chosen from DCR Model in Table 4 and the parameters relevant to the primary electron are directly fitted with the constraints of AMS-02 data. The best-fit χ^2/n is 47.26/72. The concerned parameters are given in Table 2. As seen in the table, above GeV there is only one spectral index to describe the spectra of the primary electrons, which indicates that the primary electrons have a simple power law feature connected with the origin of the astrophysical background.

N_e	γ_1^e	ρ_{br1}^e	γ_2^e
0.4198	0.8462	1.6424	2.6193

Table 2: Best-fit values of the parameters with the constraints of AMS-02 data. The units of normalization N_e is $10^{-9}\text{MeV}^{-1}\text{cm}^{-2}\text{sr}^{-1}\text{s}^{-1}$, and the referred energy of CR electrons is 34.5 GeV. The break of injection electron spectra is ρ_{br1}^e , whose unit is GV. $\gamma_{1,2}^e$ are spectral indices below/above the break, respectively.

In the fitting of annihilation cross-section of dark matter, the annihilation channels of dark matter contributing to CR electrons, positrons and antiprotons involve the following particle states:

- $2\mu, 4\mu, 2\tau, 4\tau, W^+W^-, b\bar{b}, ZZ, q\bar{q}, hh$ and $t\bar{t}$ for CR positrons and electrons

- W^+W^- , $b\bar{b}$, ZZ , hh , $q\bar{q}$ and $t\bar{t}$ for CR antiprotons

The annihilation spectra of Majorana dark matter particles via these channels are calculated using the numerical package PYTHIA v8.175 [45]. The analysis from dark matter decays is found in the paper [46].

Through the global χ^2 -fit using the MINUIT package, the best-fit values of the parameters and spectrum of CRs are derived from the minimized χ^2 . In Table 3, the best-fit parameters of each model are listed. In Table 4, the corresponding relations of the models and their concerned experimental data are presented, which shows the best-fit χ^2 values for the models with the relevant experiments.

Para.	DCR	DR	DC	DCR _V
α	8.69E-03	0.238	8.0E-3	0.0
$\phi(\phi^{e+})$	689.96	597.4(817.6)	394.8	603.5
$V_A(V_A^{e+})$	94.20	44.46		156.37(178.43)
V_{c0}	538.12		32.21	4673.1
$\frac{dV_c}{dz}$	75.27		2.57	26.2
Z_h	3.982	3.7	4.0	4.013
D_0/Z_h	2.691	1.636	1.164	21.166
δ	0.305	0.321	0.393	0.144
N_p	4.589	4.533	4.53	4.564
ρ_{br}	7.001	10.153	8.41	5.032
γ_1^p	1.828	1.772	1.748	1.654
γ_2^p	2.410	2.447	2.427	2.411

Table 3: The best-fit parameters of models DCR, DR and DC. The units of N_p are $10^{-9}\text{MeV}^{-1}\text{cm}^{-2}\text{sr}^{-1}\text{s}^{-1}$. ϕ , ρ_{br} , Z_h , D_0/Z_h , v_A and V_{c0} are in units of MV, GV, kpc, $10^{28}\text{cm}^2\text{s}^{-1}/\text{kpc}$, km s^{-1} and km s^{-1} . In DR model, the bracketed ϕ^{e+} or V_A^{e+} is only used for CR positrons. The rest propagation parameters are referred to the example 01 of GALPROP WebRun [47].

4 Results

In Table 3, the parameters of all models are listed. These parameters are the best-fit values in the χ^2 fitting by using the MINUIT package. In all the models, the propagation parameters relevant to the injection spectra of CR nucleons have only slight differences between the models. The best-fit values for α are less than 1 in all models. In fact,

α approaches to vanish in the DCR and DC models, which indicates that the injection spectra of CR nucleons become very sharp near the referred rigidity. The strong constraint is derived from the latest released B/C data at AMS-02 experiment [15].

In Table 4, the best-fit χ^2 relevant to the three types of model DCR, DR and DC are given. With the total χ^2 over the point numbers of the experimental data, DC and DR models are assessed to not fit to AMS-02 data. The lately released B/C data get higher precision and lead to a more complex feature of spectra than the other experimental data, which makes fitting become more stringent. As a consequence, the relevant χ^2 dominates in the total χ^2 . It is shown that the DC model that does not include the re-acceleration term in the propagation equation(1), leads the flux of CR protons, B/C and antiprotons to deviate from AMS-02 data. On the contrary, when excluding the convection term and only considering the re-acceleration effect, i.e., the so-called DR model, which is found to result in an inconsistent prediction for the flux of CR positrons. Even if the solar modulations are separately considered for CR positrons and nucleons in the DR model, the tension between the measured and the predicted flux of CR positrons cannot be relaxed in the low energies. It is noted that in the DR model the values χ^2 relevant to P, B/C and antiproton are less than the point numbers of AMS-02 data, which implies that the re-acceleration diffuse model may be used to predict the flux of antiprotons. In fact, with an alternative calculation by using MC generators and Z-factors [34, 38], we find that the flux of CR antiprotons can well be fitted to the AMS-02 data and the access of CR antiprotons can be eliminated in the low energies.

Models	$\chi^2_{P,N=72}$	$\chi^2_{B/C,N=67}$	$\chi^2_{P,N=10}$	$\chi^2_{e^+,N=16}$	$\chi^2_{N=165}$	$\chi^2_{N=165}/N$
DCR	27.57	55.13	15.96	18.68	117.33	0.71
DR	47.02	288.31	8.74	117.27	461.33	2.8
DC	424.6	414	594.5	1037.33	2470.43	14.97
DCR _V	14.12	77.77	17.51	14.32	123.72	0.75

Table 4: The best-fit χ^2 relevant to the models DCR, DR and DC. the subscript N of χ^2 denotes the number of the experiment data points, for instance, the number of AMS-02 proton data points is N=72. The total χ^2 and its value over the total data-points of the chosen experiment for each model are presented in the two tail columns.

As seen in Table 4, the over-predicted flux of CR positrons is not well depressed until the convection term is added to the DR model, i.e. the so-called DCR model. In the conventional model, the potential ϕ of the solar modulation is once taken to be different for the CR positrons and nucleons. In DCR model, the prediction for CR positron flux has been well improved without taking different ϕ . At the same time, the under-predicted

flux of CR antiprotons is enhanced, so that the resulting flux is simultaneously consistent with the AMS-02 data at the low energies. In the DCR_V model, Alfvén speed V_A has the two different values relevant to CR positrons and CR nucleons, which are found in Table 3. Comparing χ^2 between the DCR and DCR_V models in Table 4, it is found that the differences of re-acceleration effect does not apparently improve the fluxes of CR positrons and CR nucleons to fit to AMS-02 data. At the meantime, as a bad result, the Galactic wind velocity V_c and the diffusion coefficient D_0 are converged into the large values.

It is known that the spectra of CR protons from the measurement of AMS-02 experiment have two breaks of power index with the kinetic energy increasing from 0.5 GeV to 2 TeV [12]. The second break of the CR proton spectra means that the absolute index of CR proton spectra begin to decrease above 330 GeV, which is often called as CR hardening. From a comparison of χ^2 for the CR protons in Table 4, it is indicated that the flux of CR protons with the multiple power indices may be well predicted and derived from the re-acceleration and convection processes considered here. Though the DCR_V model does not help to improve the prediction of the fluxes of CR positrons and antiprotons, the large V_c and D_0 promote the χ^2 relevant to CR protons decreasing from 27.57 to 14.12. The experimental data of CR protons with high precision from AMS-02 has 72 points. The χ^2 14.12 means the flux of CR protons is better predicted in the DCR_V model, which justifies the convection effect for CR propagation.

On the left of the first row of Figure 1, the fluxes of CR protons are drawn. It is apparently seen that the fluxes of CR protons above 330 GeV have different trends changing with different models. As a result of the comparison among the models, DCR model can well predict the hardening flux of CR protons and the flux at the low energies is also well consistent with the AMS-02 data, which distinguishes from the DR model.

On the right of the first row in Figure 1, the ratio of Boron to Carbon flux in the DC model is inconsistent with the AMS-02 data below 2 GeV, which indicates that the DC model cannot give a significant prediction.

In Figure 1, the fluxes of CR antiprotons are plotted at the left of the second row. From a low to high energy, except for the DC and DCR_0 models, the DCR and DR models lead to a consistent prediction for the flux of CR antiprotons though the tail data of AMS-02 show a bulge that cannot completely be fitted. At the low energies, the best-fit flux of CR antiprotons prevents the access interpretation in many existing papers, which can be seen from the flux of CR antiprotons predicted with the DCR_0 model that is relevant to a conventional hadronic interaction model. In some papers, the access flux was interpreted as the contribution from dark matter annihilation. Nevertheless, at the high energies, the bulge relative to the predicted flux of CR antiprotons still exists and

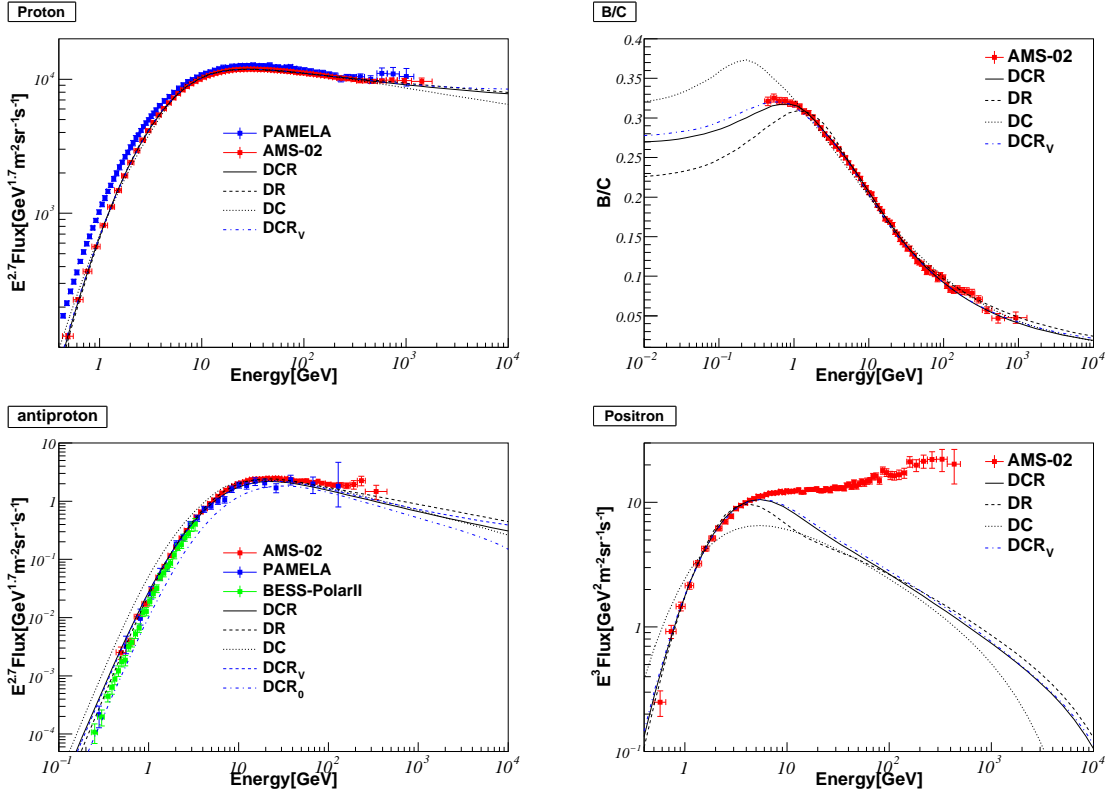


Figure 1: In the first row, the flux of CR protons (left) predicted from the models DCR, DR and DC in comparison with the measurements from AMS-02 [12] and PAMELA [48] experiments; the ratio of Boron to Carbon flux (right) predicted from the models: DCR, DR and DC, and the measurements from AMS-02 [15] experiment. In the second row, the flux of CR antiprotons (left) and CR positrons (right) predicted from the models: DCR(DCR₀), DR and DC, and the measurements from AMS-02 [13, 14, 49], PAMELA [50] and BESS-PolarII [51] experiments. DCR₀ model is relevant to the conventional hadronic interaction models and does not use the expression in Equation (11).

needs a further interpretation. We shall make a detailed analysis in next section.

On the right of the second row in Figure 1, the fluxes of CR positrons in the DCR model can well fit to the AMS-02 data at the low energies. In contrast, the DC and DR models lead to an under-predicted and over-predicted flux of CR positrons, respectively. The maximal energy range of CR positrons that can well be fitted to the AMS-02 data is up to about 10 GeV. Above 10 GeV, the CR positron excess becomes significant and begins to be enlarged with the energy increasing. It implies that new sources, different from the secondary particle production, need to be brought in for an additional contribution to CR positrons. In the next section, a possible dark matter interpretation of positron excess will be discussed.

In Figure 2, all of the figures are drawn with the data calculated using DCR model. On the left of the second row, the upper limits on the annihilation cross-sections of dark matter contributing to CR antiprotons are drawn. It is seen that the annihilation cross-sections of dark matter are different completely from our previous paper [30]. In the whole mass of dark matter, the annihilation cross-sections are greater than the predicted values from Fermi-LAT. That situation is relevant to the flux of CR antiprotons fitting to AMS-02 data at the low energies and weaker than AMS-02 data at the high energies. Based on the change of χ^2 with dark matter mass on the left figure of last row, the masses of dark matter are chosen by referring to the minimal χ^2 . The flux of CR antiprotons from the total contribution of astrophysical background and dark matter annihilation are drawn on the left of the second row. From the contribution for all channels, there are no matching fluxes of the last second point of AMS-02 data. This is because the annihilation spectra of dark matter contributing to CR antiprotons are not sharp as the CR electrons. Thus, the slight bulge in the tail data of AMS-02 does not strongly constrain the interpretations of dark matter contributing to CRs. However, for the positron excess, the situation is changed completely.

As seen on the right of Figure 2, the upper limits on the annihilation cross-sections of dark matter contributing to CR electrons and positrons, the total flux of CR electrons and positrons and the χ^2 relevant to the total of CR electrons and positrons are drawn, respectively, in the first, second and last rows. In our present consideration, the analysis of positron excess is based on the total fluxes of CR electrons and positrons, which is different from the CR positron flux or fraction data of AMS-02 used in the previous papers. The compatibility of the large annihilation cross section with the thermal relic density is discussed in terms of self-interacting DM [21, 22, 52–55, 55] and in connection with collider physics [56, 57]. Being similar to the CR antiprotons, the astrophysical backgrounds of the total electrons and positrons are also calculated by using DCR model. Based on the model, the injection spectra of the primary electrons are best-fit to the $e^- - e^+$ data of AMS-02 and the relevant power indices are found in Table 2. Apparently, based on the redefined background of CR electrons, the total fluxes of CR electrons and positrons also have the excesses to the CR background. On the right figure of second row, the flux of background is well consistent with the AMS-02 data at the low energies, but at the high energies, the experimental data of AMS-02 are manifestly in excess of the background.

In the first row of Figure 2, the upper limits on the annihilation cross-sections of dark matter contributing to CR electrons and positrons via many channels: 2μ , W^+W^- , etc, are plotted. As seen from the figure, the upper limits relevant to the lepton channels are different from the other channels with mass of dark matter increasing and the trend

differences between them are remarkable. The cross masses of dark matter between the channels are from the several to 10 TeV, where the same annihilation cross-sections appear. In the last row of Figure 2, the best-fit masses of dark matter are found easily from the change of χ^2 with the mass of dark matter increasing. Except for 2μ and 4μ final states, the χ^2 are less than the twice of the experimental data points, and the predicted masses of dark matter are from 794 GeV to 11 TeV. The annihilation of heaviest dark matter is via the $t\bar{t}$ final state and the lightest one is relevant to 2τ . The total fluxes of CR electrons and positrons from the background and dark matter annihilation are drawn in the second row of Figure 2. As seen in the figure, at the high energies the predicted fluxes of CR electrons and positrons are consistent with AMS-02 data and the best fluxes fitting to AMS-02 data are relevant to the W^+W^- final state.

In this paper, as the excess is relevant to the experimental measurement of CR electrons and positrons with ignoring the charge polarity, the interpretation of the excess is easy to be promoted at higher energies for the upcoming data of DAMPE satellite experiment.

5 Conclusions

In the re-acceleration diffusion model, the propagation parameters were shown to be well constrained only with CR protons and B/C data of AMS-02 in our previous paper [16]. However, based on those parameter models, the predicted fluxes of CR positrons and antiprotons at the low energies deviate significantly from the current AMS-02 data. In the past analyses by many groups, the situation could not be improved completely. The analysis in ref. [24] indicated that the under-predicted antiprotons may result from a general feature of the re-acceleration models. In our present considerations, the CR antiproton productions have been recalculated by using MC generators and Z-factors [34, 38]. As a consequence, in the re-acceleration diffusion model, the under-predicted flux of CR antiprotons can be enhanced to fit consistently the AMS-02 data.

For the CR positrons, as shown in Fig.10 of ref. [59], the over-predicted flux could not be improved by using the MC generator: FLUKA [7, 8]. In this paper, by using the diffusion model with including both the convection and re-acceleration contributions, the over-predicted flux of CR positrons has been shown to be depressed. In the conventional model, the potential of the solar modulation is taken to be the same for the CR positrons and nucleons. In re-acceleration diffusion model, it has been shown that the prediction of CR positron flux can not be improved even if the solar modulation is made to be different for the CR positrons and nucleons.

In the further exploration on the tension between fluxes of CR positrons and nucleons

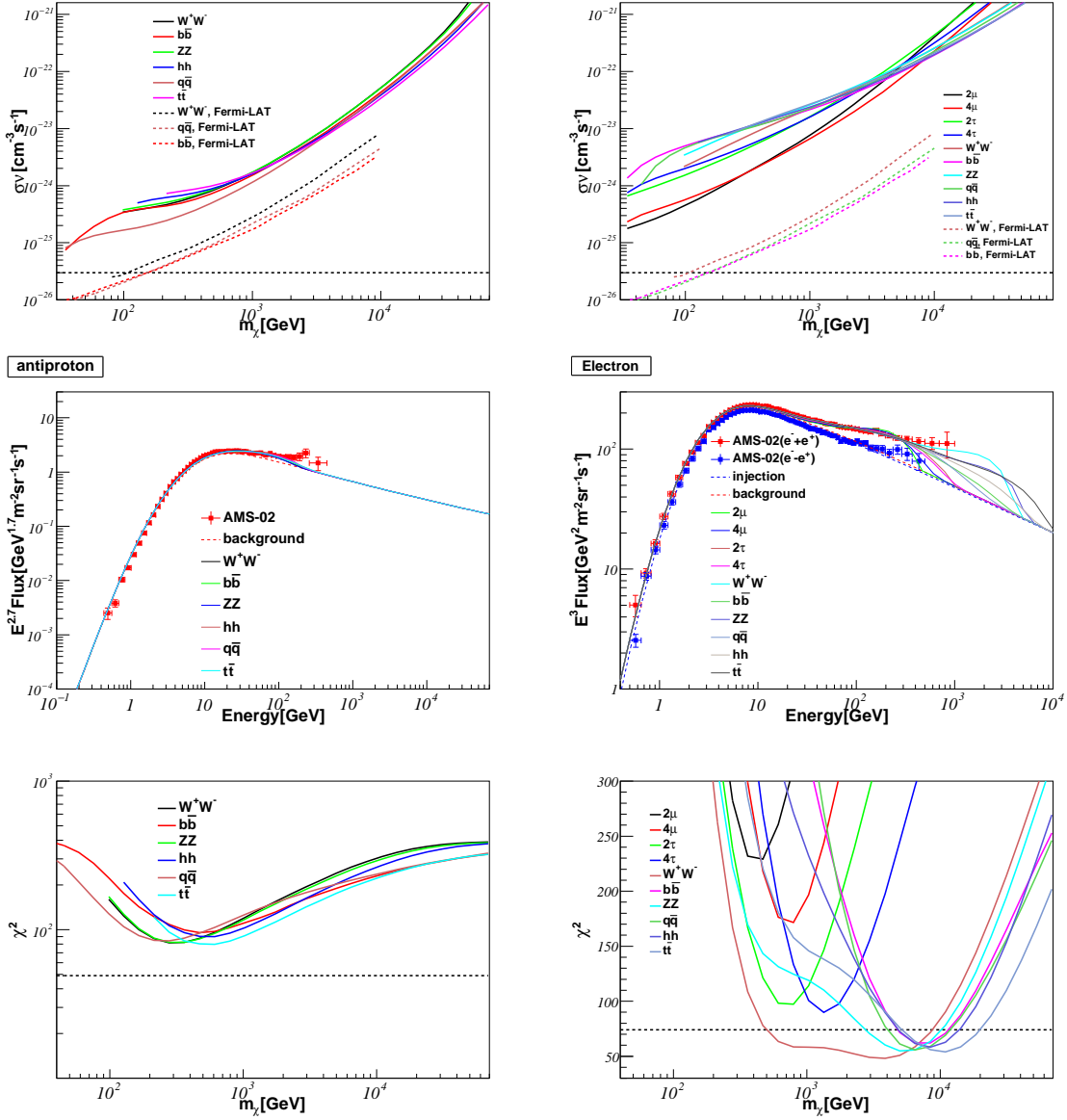


Figure 2: All of rows: the left for CR antiprotons and the right for the total of CR electrons and positrons. At the first row, upper limits on the annihilation cross-sections of dark matter via the channels of $b\bar{b}$, etc. The dash-line denotes the thermal cross-section $3 \times 10^{-26} \text{cm}^3 \text{s}^{-1}$. The upper limits on the $q\bar{q}$, $b\bar{b}$ and W^+W^- channels from the Fermi-LAT 6-year gamma-ray data of dwarf spheroidal satellite galaxies of the Milky Way are also shown [58]. At the second row, the fluxes of CRs relevant to the astrophysical background, dark matter and AMS-02 experiments [13, 14, 49]. ($e^- - e^+$) denotes the primary electrons. ($e^- + e^+$) denotes CR electrons and positrons. At the last row, χ^2 change with the mass of dark matter increasing. The dash-line denotes number of the experimental data points.

predicted by propagation models, it has been demonstrated that when the processes of re-acceleration and convection in the propagation of CRs are both included, such a tension can be relaxed completely, and the predicted fluxes for CR positrons, antiprotons and protons are remarkably consistent with the latest AMS-02 data. In particular, the flux of CR protons with the hardening feature above 330 GeV can well be predicted.

Based on the predicted background of CR positrons and antiprotons, the contribution to CRs from dark matter is analyzed. For CR antiprotons, the slight bulge in the tail data of AMS-02 do not strongly constrain the interpretations of dark matter contributing to CRs. the upper limits on the annihilation cross-sections of dark matter contributing to CR antiprotons are constrained with the latest AMS-02 data. The result indicate that the annihilation cross-sections of dark matter are different completely from the previous papers including the other groups. In the whole mass of dark matter, the annihilation cross sections are enhanced.

Our analysis on the positron excess is based on the total fluxes of CR electrons and positrons, which is different from the CR positron flux or fraction data of AMS-02 adopted in the previous published papers. The injection spectra of the primary electrons are best-fit to the $e^- - e^+$ data of AMS-02. As a consequence, based on the redefined background of CR electrons, the total fluxes of CR electrons and positrons are manifestly in excess of CR background.

For the excess of the total fluxes of CR electrons and positrons, the upper limits relevant to the lepton channels have been shown to be different from other channels with mass of dark matter increasing. The cross masses of dark matter among all channels are found to range from several to 10 TeV, where the same annihilation cross-sections appear. Except for 2μ and 4μ final states, the χ^2 are less than the twice of the experimental data points, and the predicted masses of dark matter are from 794 GeV to 11 TeV. The annihilation of heaviest dark matter is through the $t\bar{t}$ final state and the lightest one is via the 2τ channel.

It has been shown that the excess is relevant to the experimental measurements of CR electrons and positrons with ignoring the charge polarity, the interpretation of the excess can easily be extended to analyze the upcoming data of DAMPE satellite experiment in a high energy region.

Acknowledgments

Y. L. W. is grateful to S. Ting for insightful discussions. We thank P. Zuccon, A. Kounine, A. Oliva, and S. Haino for helpful discussions on the details of the AMS-02 detector. This work is supported in part by the National Basic Research Program of China (973

Program) under Grant No. 2010CB833000; and the National Nature Science Foundation of China (NSFC) under Grants No. 11335012, No. 11475237 and No. 11121064, and also by the Strategic Priority Research Program of the Chinese Academy of Sciences, Grant No. XDB23030100 as well as the CAS Center for Excellence in Particle Physics (CCEPP). The numerical calculations were done using the HPC Cluster of SKLTP/ITP-CAS.

References

- [1] E. Fermi, *On the Origin of the Cosmic Radiation*, *Physical Review* **75** (apr, 1949) 1169–1174.
- [2] G. Krymskii, *A regular mechanism for the acceleration of charged particles on the front of a shock wave*, *Akademiia Nauk SSSR Doklady* **234** (1977) 1306–1308.
- [3] R. D. Blandford and J. P. Ostriker, *Particle acceleration by astrophysical shocks*, *The Astrophysical Journal* **221** (apr, 1978) L29.
- [4] L. O. Drury, *An introduction to the theory of diffusive shock acceleration of energetic particles in tenuous plasmas*, *Reports on Progress in Physics* **46** (aug, 1983) 973–1027.
- [5] R. Blandford and D. Eichler, *Particle acceleration at astrophysical shocks: A theory of cosmic ray origin*, *Physics Reports* **154** (oct, 1987) 1–75.
- [6] M. Amenomori et al., *The AllParticle Spectrum of Primary Cosmic Rays in the Wide Energy Range from 10 14 to 10 17 eV Observed with the TibetIII AirShower Array*, *The Astrophysical Journal* **678** (may, 2008) 1165–1179, [[arXiv:0801.1803](#)].
- [7] A. Ferrari, P. Sala, A. Fasso, and J. Ranft, *FLUKA: A Multi-Particle Transport Code*, tech. rep., Stanford Linear Accelerator Center (SLAC), Menlo Park, CA, dec, 2005.
- [8] T. T. Bohlen, F. Cerutti, M. P. W. Chin, A. Fasso, A. Ferrari, P. G. Ortega, A. Mairani, P. Sala, G. Smirnov, and V. Vlachoudis, *The FLUKA Code: Developments and Challenges for High Energy and Medical Applications*, *Nuclear Data Sheets* **120** (2014).
- [9] S. Ostapchenko, *Monte Carlo treatment of hadronic interactions in enhanced Pomeron scheme: I. QGSJET-II model*, *Physical Review D* **83** (oct, 2010) 014018, [[arXiv:1010.1869](#)].
- [10] T. Pierog, I. Karpenko, J. M. Katzy, E. Yatsenko, and K. Werner, *EPOS LHC: Test of collective hadronization with data measured at the CERN Large Hadron Collider*, *Physical Review C* **92** (sep, 2015) 034906, [[arXiv:1306.0121](#)].
- [11] V. S. Berezinskii, S. V. Bulanov, V. A. Dogiel, and V. L. Ginzburg, *Astrophysics of cosmic rays*. North-Holland, Amsterdam, 1990.

- [12] M. Aguilar et al., *Precision Measurement of the Proton Flux in Primary Cosmic Rays from Rigidity 1 GV to 1.8 TV with the Alpha Magnetic Spectrometer on the International Space Station*, *Physical Review Letters* **114** (apr, 2015) 171103.
- [13] M. Aguilar et al., *Electron and Positron Fluxes in Primary Cosmic Rays Measured with the Alpha Magnetic Spectrometer on the International Space Station*, *Physical Review Letters* **113** (sep, 2014) 121102.
- [14] M. Aguilar et al., *Antiproton Flux, Antiproton-to-Proton Flux Ratio, and Properties of Elementary Particle Fluxes in Primary Cosmic Rays Measured with the Alpha Magnetic Spectrometer on the International Space Station*, *Physical Review Letters* **117** (aug, 2016) 091103.
- [15] M. Aguilar et al., *Precision Measurement of the Boron to Carbon Flux Ratio in Cosmic Rays from 1.9 GV to 2.6 TV with the Alpha Magnetic Spectrometer on the International Space Station*, *Physical Review Letters* **117** (nov, 2016) 231102.
- [16] H.-B. Jin, Y.-L. Wu, and Y.-F. Zhou, *Cosmic ray propagation and dark matter in light of the latest AMS-02 data*, *Journal of Cosmology and Astroparticle Physics* **2015** (sep, 2015) 049–049, [arXiv:1410.0171].
- [17] O. Adriani et al., *A statistical procedure for the identification of positrons in the PAMELA experiment*, *Astroparticle Physics* **34** (jan, 2010) 1–11, [arXiv:1001.3522].
- [18] The Fermi LAT Collaboration, M. Ackermann et al., *Measurement of separate cosmic-ray electron and positron spectra with the Fermi Large Area Telescope*, *Physical Review Letters* **108** (sep, 2011) 011103, [arXiv:1109.0521].
- [19] L. Accardo et al., *High Statistics Measurement of the Positron Fraction in Primary Cosmic Rays of 0.5 - 500 GeV with the Alpha Magnetic Spectrometer on the International Space Station*, *Physical Review Letters* **113** (sep, 2014) 121101.
- [20] H.-B. Jin, Y.-L. Wu, and Y.-F. Zhou, *Implications of the first AMS-02 measurement for dark matter annihilation and decay*, *Journal of Cosmology and Astroparticle Physics* **2013** (nov, 2013) 026–026, [arXiv:1304.1997].
- [21] Z.-P. Liu, Y.-L. Wu, and Y.-F. Zhou, *Sommerfeld enhancements with vector, scalar and pseudoscalar force-carriers*, *Physical Review D* **88** (may, 2013) 096008, [arXiv:1305.5438].

- [22] J. Chen, Z.-L. Liang, Y.-L. Wu, and Y.-F. Zhou, *Long-range self-interacting dark matter in the Sun*, *Journal of Cosmology and Astroparticle Physics* **2015** (may, 2015) 021–021, [[arXiv:1505.0403](#)].
- [23] Y.-F. Zhou, *Implications of the AMS-02 data for dark matter and cosmic-ray propagation*, *PoS DSU2015* (2016) 22.
- [24] R. Trotta, G. Jóhannesson, I. V. Moskalenko, T. A. Porter, R. Ruiz de Austri, and A. W. Strong, *Constraints on cosmic-ray propagation models from a global Bayesian analysis*, *The Astrophysical Journal* **729** (mar, 2011) 106, [[arXiv:1011.0037](#)].
- [25] A. W. Strong, I. V. Moskalenko, and O. Reimer, *Diffuse Continuum Gamma Rays from the Galaxy*, *The Astrophysical Journal* **537** (jul, 2000) 763–784, [[9811296](#)].
- [26] G. Giesen, M. Boudaud, Y. Genolini, V. Poulin, M. Cirelli, P. Salati, and P. D. Serpico, *AMS-02 antiprotons, at last! Secondary astrophysical component and immediate implications for Dark Matter*, [arXiv:1504.0427](#).
- [27] R. Kappl, A. Reinert, and M. W. Winkler, *AMS-02 Antiprotons Reloaded*, *Journal of Cosmology and Astroparticle Physics* **2015** (jun, 2015) 034–034, [[arXiv:1506.0414](#)].
- [28] S.-J. Lin, X.-J. Bi, P.-F. Yin, and Z.-H. Yu, *Implications for dark matter annihilation from the AMS-02 antiproton / p ratio*, [arXiv:1504.0723](#).
- [29] D. Hooper, T. Linden, and P. Mertsch, *What does the PAMELA antiproton spectrum tell us about dark matter?*, *Journal of Cosmology and Astroparticle Physics* **2015** (mar, 2015) 021–021, [[arXiv:1410.1527](#)].
- [30] H.-B. Jin, Y.-L. Wu, and Y.-F. Zhou, *Upper limits on DM annihilation cross sections from the first AMS-02 antiproton data*, *Physical Review D* **92** (sep, 2015) 055027, [[arXiv:1504.0460](#)].
- [31] H.-B. Jin, Y.-L. Wu, and Y.-F. Zhou, *Implications of the first AMS-02 antiproton data for dark matter*, *International Journal of Modern Physics A* **30** (oct, 2015) 1545008, [[arXiv:1508.0684](#)].
- [32] M.-Y. Cui, Q. Yuan, Y.-L. S. Tsai, and Y.-Z. Fan, *A possible dark matter annihilation signal in the AMS-02 antiproton data*, [arXiv:1610.0384](#).

- [33] X.-J. Huang, C.-C. Wei, Y.-L. Wu, W.-H. Zhang, and Y.-F. Zhou, *Antiprotons from dark matter annihilation through light mediators and a possible excess in AMS-02 p/\bar{p} data*, [arXiv:1611.0198](#).
- [34] M. Kachelriess, I. V. Moskalenko, and S. S. Ostapchenko, *New calculation of antiproton production by cosmic ray protons and nuclei*, *The Astrophysical Journal* **803** (feb, 2015) 54, [[arXiv:1502.0415](#)].
- [35] E. C. Stone, A. C. Cummings, F. B. McDonald, B. C. Heikkila, N. Lal, and W. R. Webber, *Voyager 1 Observes Low-Energy Galactic Cosmic Rays in a Region Depleted of Heliospheric Ions*, *Science* **341** (jul, 2013) 150–153.
- [36] C. Corti, V. Bindi, C. Consolandi, and K. Whitman, *Solar Modulation of the Proton Local Interstellar Spectrum with AMS-02, Voyager 1 and PAMELA*, [arXiv:1511.0879](#).
- [37] L. J. Gleeson and W. I. Axford, *Solar Modulation of Galactic Cosmic Rays*, *The Astrophysical Journal* **154** (dec, 1968) 1011.
- [38] M. Kachelriess, I. V. Moskalenko, and S. S. Ostapchenko, *Nuclear enhancement of the photon yield in cosmic ray interactions*, *The Astrophysical Journal* **789** (may, 2014) 136, [[arXiv:1406.0035](#)].
- [39] E. S. Seo and V. S. Ptuskin, *Stochastic reacceleration of cosmic rays in the interstellar medium*, *The Astrophysical Journal* **431** (aug, 1994) 705.
- [40] A. W. Strong and I. V. Moskalenko, *Propagation of CosmicRay Nucleons in the Galaxy*, *The Astrophysical Journal* **509** (dec, 1998) 212–228, [[9807150](#)].
- [41] S. Kelner, F. Aharonian, and V. Bugayov, *Energy spectra of gamma rays, electrons, and neutrinos produced at proton-proton interactions in the very high energy regime*, *Physical Review D* **79** (feb, 2009) 039901, [[0606058](#)].
- [42] I. V. Moskalenko and A. W. Strong, *Production and Propagation of CosmicRay Positrons and Electrons*, *The Astrophysical Journal* **493** (feb, 1998) 694–707, [[9710124](#)].
- [43] I. V. Moskalenko, A. W. Strong, J. F. Ormes, and M. S. Potgieter, *Secondary antiprotons and propagation of cosmic rays in the Galaxy and heliosphere*, *The Astrophysical Journal* **565** (jun, 2001) 280–296, [[0106567](#)].

- [44] D. Chen, J. Huang, and H.-B. Jin, *SPECTRA OF COSMIC RAY ELECTRONS AND DIFFUSE GAMMA RAYS WITH THE CONSTRAINTS OF AMS-02 AND HESS DATA*, *The Astrophysical Journal* **811** (oct, 2015) 154, [arXiv:1412.2499].
- [45] T. Sjöstrand, S. Mrenna, and P. Skands, *A brief introduction to PYTHIA 8.1*, *Computer Physics Communications* **178** (2008), no. 11 852–867, [arXiv:0710.3820].
- [46] Y. Mambrini, S. Profumo, and F. S. Queiroz, *Dark Matter and Global Symmetries*, *Physics Letters B* **760** (aug, 2015) 807–815, [arXiv:1508.0663].
- [47] A. Vladimirov, S. Digel, G. Jóhannesson, P. Michelson, I. Moskalenko, P. Nolan, E. Orlando, T. Porter, and A. Strong, *GALPROP WebRun: An internet-based service for calculating galactic cosmic ray propagation and associated photon emissions*, *Computer Physics Communications* **182** (may, 2011) 1156–1161, [arXiv:1008.3642].
- [48] O. Adriani and Others, *PAMELA Measurements of Cosmic-ray Proton and Helium Spectra*, *Science* **332** (2011) 69–72, [arXiv:1103.4055].
- [49] M. Aguilar et al., *Precision Measurement of the ($e^+ + e^-$) Flux in Primary Cosmic Rays from 0.5 GeV to 1 TeV with the Alpha Magnetic Spectrometer on the International Space Station*, *Physical Review Letters* **113** (nov, 2014) 221102.
- [50] O. Adriani et al., *PAMELA results on the cosmic-ray antiproton flux from 60 MeV to 180 GeV in kinetic energy*, *Physical Review Letters* **105** (sep, 2010) 121101, [arXiv:1007.0821].
- [51] K. Abe et al., *Measurement of the cosmic-ray antiproton spectrum at solar minimum with a long-duration balloon flight over Antarctica*, *Physical Review Letters* **108** (jul, 2011) 051102, [arXiv:1107.6000].
- [52] Z.-P. Liu, Y.-L. Wu, and Y.-F. Zhou, *Dark matter conversion as a source of boost factor for explaining the cosmic ray positron and electron excesses*, *Journal of Physics: Conference Series* **384** (dec, 2011) 012024, [arXiv:1112.4030].
- [53] T. Li, S. Miao, and Y.-F. Zhou, *Light mediators in dark matter direct detections*, *Journal of Cosmology and Astroparticle Physics* **2015** (dec, 2014) 032–032, [arXiv:1412.6220].
- [54] T. Li and Y.-F. Zhou, *Strongly first order phase transition in the singlet fermionic dark matter model after LUX*, *Journal of High Energy Physics* **2014** (feb, 2014) 6, [arXiv:1402.3087].

- [55] Z.-L. Liang, Y.-L. Wu, Z.-Q. Yang, and Y.-F. Zhou, *On the evaporation of solar dark matter: spin-independent effective operators*, *Journal of Cosmology and Astroparticle Physics* **2016** (jun, 2016) 018–018, [[arXiv:1606.0215](#)].
- [56] X.-J. Huang, W.-H. Zhang, and Y.-F. Zhou, *A 750 GeV dark matter messenger at the Galactic Center*, *Physical Review D* **93** (dec, 2015) 115006, [[arXiv:1512.0899](#)].
- [57] X.-J. Huang, W.-H. Zhang, and Y.-F. Zhou, *Connecting the LHC diphoton excess to the Galactic center gamma-ray excess*, *Physical Review D* **94** (may, 2016) 035019, [[arXiv:1605.0901](#)].
- [58] F.-L. Collaboration, *Searching for Dark Matter Annihilation from Milky Way Dwarf Spheroidal Galaxies with Six Years of Fermi-LAT Data*, *Physical Review Letters* **115** (mar, 2015) 231301, [[arXiv:1503.0264](#)].
- [59] M. Mazziotta, F. Cerutti, A. Ferrari, D. Gaggero, F. Loparco, and P. Sala, *Production of secondary particles and nuclei in cosmic rays collisions with the interstellar gas using the FLUKA code*, *Astroparticle Physics* **81** (aug, 2016) 21–38, [[arXiv:1510.0462](#)].